Journal of Energy Technology
Vol. 18, No. 1, pp. 21–34, May 2025

Original Scientific Article

Artificial Intelligence - Based Exergy Analysis of an Absorption Cooling System

Submitted
2. 4. 2025

Accepted
7. 4. 2025

Published
30. 5. 2025

Dušan Strušnik
nergetika Ljubljana d.o.o., TE-TOL Unit, Ljubljana, Slovenia
dusan.strusnik@gmail.com

Corresponding Author
dusan.strusnik@gmail.com

Abstract An artificial intelligence (AI)-based exergy analysis of an absorption cooling system (ACS), utilizing a lithium bromide–water refrigeration cycle, is presented in this paper. The ACS is characterised by the utilisation of the intermediate-pressure (IP) extraction steam from the steam turbine for its operation. The exergy analysis of the ACS is detailed, based on AI modelling through a machine learning algorithm, which predicts and optimises the ACS performance. The machine learning algorithm is validated using real process data obtained through ACS measurements via the supervisory control and data acquisition (SCADA) system. The AI results show that the ACS generates 126.71 kW of cooling for district cooling and 279.57 kW of heat, which is used for heating demineralised water. During the analysis period, the ACS consumed an average of 152.86 kW of IP steam, and operated with an average exergy efficiency of 17.3%. The study suggests that the average exergy efficiency of the ACS could be improved by using lower-quality steam, or even hot water, for operation.

Keywords
absorption,
analysis,
Artificial Intelligence,
cooling,
efficiency,
exergy

https://doi.org/10.18690/jet.18.1.21-34.2025

University of Maribor Press

1 Introducton

An absorption cooling system (ACS) is a type of refrigeration system that uses heat energy instead of electricity to produce cooling. Cold is produced with the help of heat, and involves key components such as a generator, condenser, absorber, evaporator, and auxiliary devices like pumps, heat exchangers and cooling towers [1]. A schematic representation of the ACS operation is shown in Fig. 1.

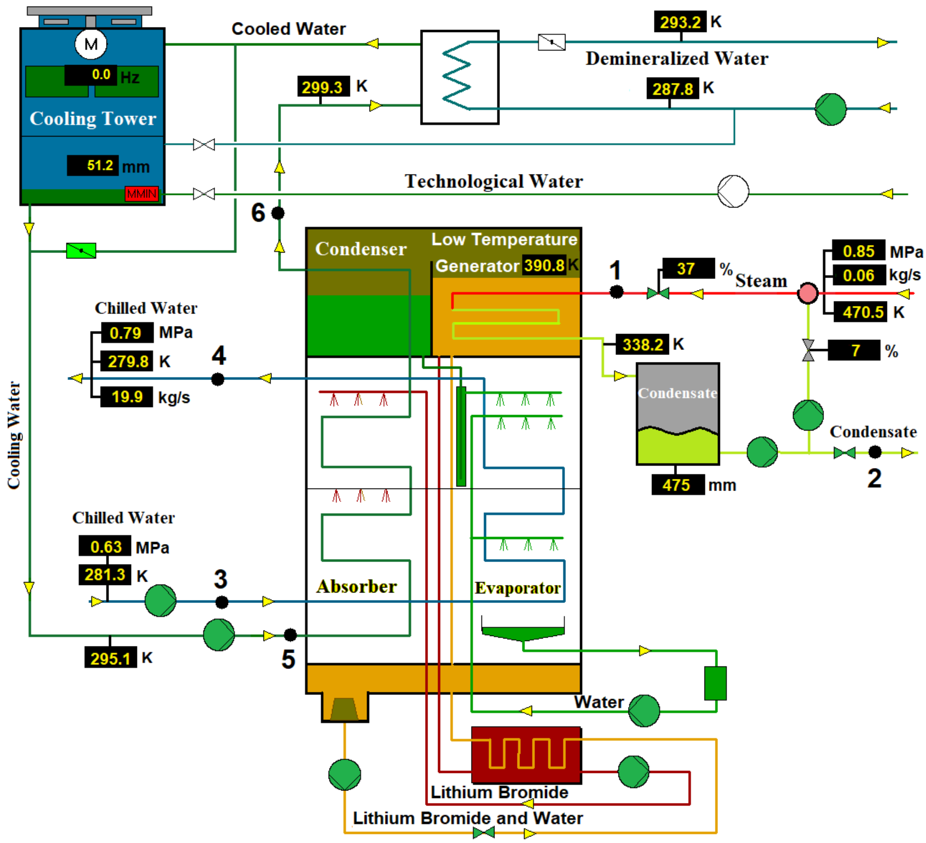

Figure 1: Schematic representation of the operation of the ACS [2]

The ACS analysed in this study utilises lithium bromide as the absorbent and water as the refrigerant. Water is considered an ideal natural refrigerant, due to its safety, wide availability and low cost, while lithium bromide offers key properties such as stability in aqueous solutions and low vapour pressure under absorber conditions.

In the ACS cycle, the lithium bromide–water solution is pumped from the absorber to the low-temperature generator, where it is heated using intermediate-pressure extraction steam from the steam turbine. Upon reaching the evaporation temperature, the water vapour is separated from the solution, thereby increasing the lithium bromide concentration. The separated vapour flows into the condenser, where it releases heat to the cooling water and condenses. The resulting condensate passes through a throttling valve, experiencing a pressure and temperature drop, before entering the evaporator. In the evaporator, the condensate evaporates by absorbing heat from the chilled water, which is, subsequently, used for district cooling. The evaporated water vapour is then absorbed back into the lithium bromide solution within the absorber, completing the cycle. A detailed description of the ACS operation is available in [3], [4]. Fig. 2 presents a schematic of the ACS integrated into the existing power plant system, highlighting the connections for district cooling and demineralised water heating.

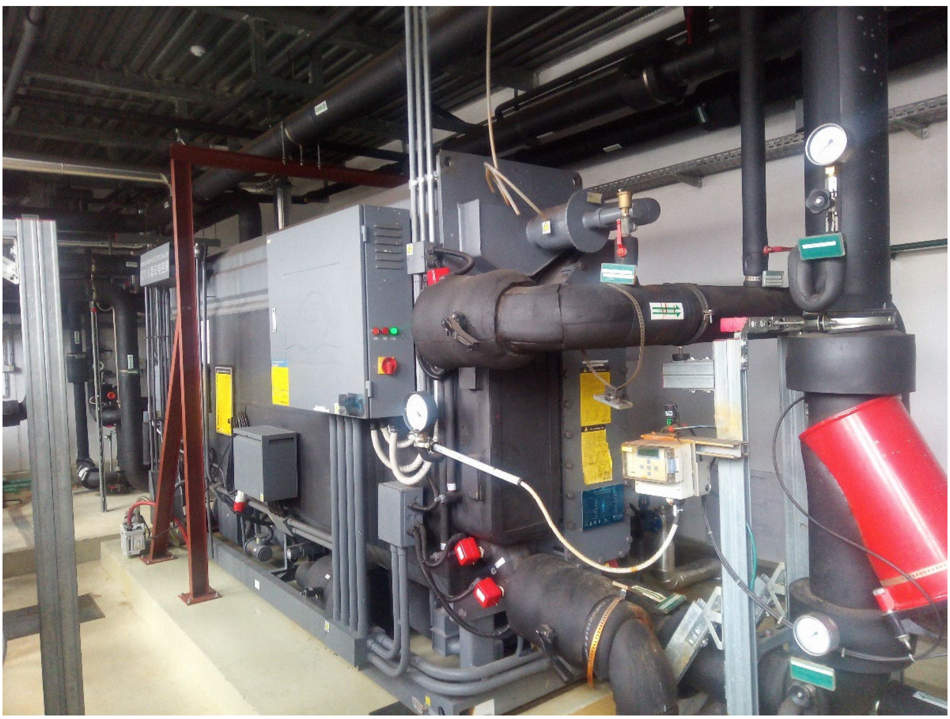

Figure 2: Integration of the ACS into the existing plant system

A significant advantage of this system is the recovery of waste heat, which would otherwise be discharged into the environment via the cooling tower. In this configuration, the recovered waste heat is utilised to preheat demineralised water, as illustrated in Figure 1. The preheated demineralised water serves as an additional feedwater source for power plant operations, enhancing the overall plant efficiency. The ACS manufacturer's nameplate is presented in Figure 3, and the operating conditions and nominal properties of the ACS are summarised in Table 1 [5].

Figure 3: ACS manufacturer's plate

Table 1: Nominal properties of the *ACS* [5]

Manufacture BS39X0.8-34/27-50			
Model	BS50	Cooled water outlet	307 K
Manufactured	07. 2008	Cooled water inlet	300 K
Cooling capacity	450 kW	Cooled water flow	26.4 kg/s
Chilled water outlet	280 K	Cooled water pressure	0.8 MPa
Chilled water inlet	285 K	Steam pressure	0.8 MPa
Chilled water flow	21.6 kg/s	Max. steam consumption	0.136 kg/s
Chilled water pressure	0.8 MPa	Voltage	400 V

2 AI-based exergy analysis and machine learning modelling of the ACS

In this section, an AI approach is applied to perform the exergy analysis and machine learning modelling of the ACS. A machine learning algorithm is developed to predict and optimise ACS performance based on real operational data collected through a SCADA system. The machine learning algorithm simulates the real behaviour of the ACS using a trained artificial neural network (ANN). The ANN is developed through three phases: training, validation and testing. In each phase, real input–output process data are used to minimise prediction errors. Various ANN architectures are tested, and the configuration with the lowest validation error, compared to real process behaviour, is selected for final implementation.

The architecture of the machine learning model consists of four main components: an input unit, neural mesh layers, an absorption calculation unit, and results reporting module. The input unit processes three groups of operational parameters: pressure, temperature and mass flow rate of the IP steam supplied to the ACS. The absorption calculation unit, based on the trained and validated ANN, predicts the cooling capacity of the ACS. The real process data used for model training and validation were obtained directly from the SCADA system. The complete architecture of the machine learning model for the ACS is illustrated in Fig. 4.

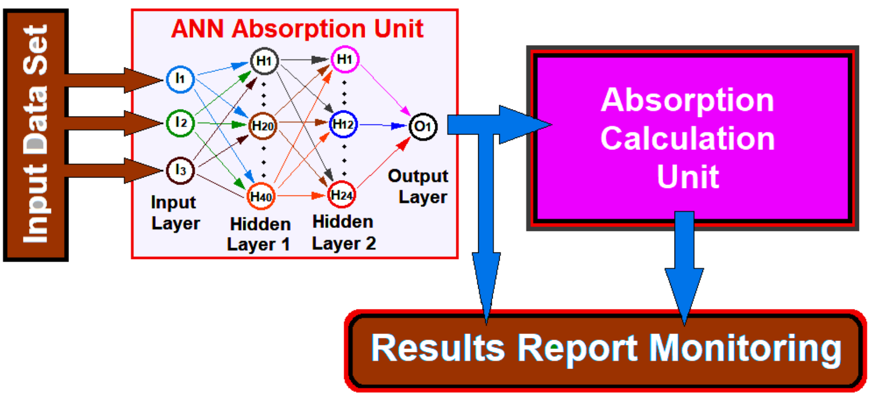

Figure 4: The architecture of the machine-learning algorithm of the ACS

The validation and training of the ANN absorption unit were conducted by testing various ANN architectures. The ANN architecture that produced the lowest prediction errors compared to the real process data was selected in the final machine-learning algorithm for the ACS. The accuracy of the ANN predictions was evaluated using different error metrics, with the mean squared error (MSE) being the most commonly used. The MSE provides a quantitative measure of the average squared difference between the predicted and actual values and is defined as [6]:

$$MSE = \frac{1}{p}\sum_{i=1}^{p}\left(t_j - o_j\right)^2 \tag{2.1}$$

whereas the root mean square error (RMSE) is defined as [6]:

$$RMSE = \left|(1/p)\sum_{j=1}^{p}\left[t_j - o_j\right]^2\right|^{1/2} \tag{2.2}$$

In addition, the correlation coefficient (R2) and mean absolute error (MAE) are respectively defined as [6]:

$$R^2 = 1 - \left[\frac{\sum_{j=1}^{p}\left(t_j - o_j\right)^2}{\sum_{j=1}^{2}\left(o_j\right)^2}\right] \tag{2.3}$$

$$MAE = \frac{1}{p}\sum_{j=1}^{p}\left|t_j - o_j\right| \tag{2.4}$$

Mean absolute percentage error (MAPE) is, respectively, defined as [6]:

$$MAPE = \frac{1}{p}\sum_{j=1}^{p}\frac{\left|t_j - o_j\right|}{t_j} \tag{2.5}$$

where t_j is the target value, o_j is the output value and p is the pattern. The correlation coefficient is normalised and ranges between 0 and 1. A very good fit yields an R^2 value of 1, whereas a poor fit results in a value near 0 [7]. The validation results of the *ANN* absorption unit algorithm structures for the selecting structure used in the machine-learning algorithm of the *ACS* are shown in Table 2.

From Table 2, it is evident (in bold) that the selecting algorithmic structure, the ANN absorption unit, has a 40-24 architecture, which means that the ANN absorption unit consists of two hidden layers. The first hidden layer contains 40 neurons, and the second hidden layer contains 24 neurons. In addition to two hidden layers, the

ANN absorption unit also contains an input layer, which contains three neurons and an output layer which contains one neuron, Fig. 4.

Table 2: Results of the validation of *ANN* absorption unit algorithmic structures

Algorithm Architecture	Epochs	Data Set Size	MAE	MAPE	MSE	RMSE	R2
ANN 60-40	41	714	0.07551	0.10692	0.01239	0.11132	0.9932
ANN 40-24	**63**	**714**	**0.06601**	**0.43904**	**0.00873**	**0.09348**	**0.9951**
ANN 10	35	714	0.08532	0.65664	0.01281	0.11318	0.9929

The absorption calculation unit contains thermodynamic equations, which calculate the thermodynamic properties, energy efficiency and exergy efficiency of the ACS. The names and values of the thermodynamic states of water and steam at individual points from Fig. 1 are shown in Table 3, where the values of specific exergy are calculated using the equation [8]:

$$e_{water\ or\ steam} = h_{water\ or\ steam} - h_0 - T_0 \cdot (s_{water\ or\ steam} - s_0) \tag{2.6}$$

where $e_{water\ or\ steam}$ is the specific exergy of the water or steam, $h_{water\ or\ steam}$ is the specific enthalpy of the water or steam, h_0 is the specific enthalpy at the ambient state, T_0 is the ambient temperature, $s_{water\ or\ steam}$ is the specific entropy of the water or steam, and s_0 is the specific entropy of the water or steam at the thermodynamic state of the environment.

Table 3: The mean values of water and steam at individual points from Fig. 1

Point	Name	Temperature (K)	Pressure (MPa)	Specific enthalpy (MJ/kg)	Specific entropy (MJ/kg)	Specific exergy (MJ/kg)
1	IP steam inlet	470	0.85	2.829	6.769•10-3	0.8484
2	IP condensate	338	0.72	0.272	0.891•10-3	0.0137
3	Chilled water inlet	281	0.5	0.033	0.119•10-3	0.0000
4	Chilled water outlet	279	0.43	0.025	0.089•10-3	0.0016
5	Cooled water inlet	295	0.30	0.092	0.323•10-3	0.0001
6	Cooled water outlet	279	0.22	0.025	0.089•10-3	0.0016

The resulting losses of the specific exergy of water and steam are calculated , thermal conductivity, internal fraction, flow losses, etc. [4]:

$$e_{loss} = \left(e_{bef} - e_{beh} - e_{usef}\right) \tag{2.7}$$

where e_{loss} are the losses of the specific exergy of the water and steam, e_{bef} is the specific exergy before the transformation of the water or steam, e_{beh} is the specific exergy behind the transformation of the water or steam, e_{usef} is the useful specific exergy. The useful specific exergy is used for district cooling (chilled water) and for demineralised water heating (cooled water). The absorption calculation unit also calculates the *ACS* exergy efficiency:

$$\eta_{ex} = \frac{e_{dem} \cdot \dot{m}_{dem} + e_{chil} \cdot \dot{m}_{chil}}{(e_{steam} - e_{cond}) \cdot \dot{m}_{steam} \cdot P_{el}} \tag{2.8}$$

where η_{ex} is the *ACS* exergy efficiency, e_{dem} is the specific exergy for the demineralised water heating, $\dot{m}_{dem}$ is the mass flow of demineralised water, e_{chil} is the specific exergy of the chilled water needed for district cooling, $\dot{m}_{chil}$ is the mass flow of the chilled water, e_{steam} is the specific exergy of the *IP* steam, e_{cond} is the specific exergy of the condensate from the *ACS*, $\dot{m}_{steam}$ is the *IP* steam mass flow required for the *ACS* operation and P_{el} is the electrical power required for the *ACS* operation. The electrical power required for *ACS* operation has ranged from 2.5 kW up to 5 kW. With the help of Eq. 9, the absorption calculation unit also calculates the exergetic coefficient of performance (*ECOP*) [9]:

$$ECOP = \frac{e_{chil} \cdot \dot{m}_{chil}}{(e_{steam} - e_{cond}) \cdot \dot{m}_{steam}} \tag{2.9}$$

where $ECOP$ is the exergetic coefficient of performance. With the help of the commonly known energy equations, the absorption calculation unit also calculates the energy thermodynamic characteristics and the coefficient of performance (*COP*) of the *ACS*. The *COP* of the *ACS* is a ratio of useful cooling provided to the energy required and is calculated by [9]:

$$COP = \frac{Q_{cold}}{Q_{oper}} \tag{2.10}$$

where Q_{cold} is the useful cold production, and the Q_{oper} is the heat required for the *ACS* operation. The useful cold production is calculated by [10]:

$$Q_{cold} = \dot{m}_{chil} \cdot c_p \cdot (T_{chil-in} - T_{chil-out}) \tag{2.11}$$

where c_p is the specific heat of the chilled water, $T_{chil-in}$ is the inlet temperature of the chilled water and $T_{chil-out}$ is the outlet temperature of the chilled water. The heat required for the *ACS* operation is calculated by[11]:

$$Q_{oper} = \dot{m}_{steam} \cdot (h_{steam-in} - h_{cond-out}) \tag{2.12}$$

where $h_{steam-in}$ is the specific enthalpy of the *IP* steam into the *ACS,* and $h_{cond-out}$ is the specific enthalpy of the condensate from the *ACS*.

3 Results of the AI-based exergy analysis

The AI-based exergy analysis of the ACS was carried out using the validated machine learning model described in the previous section. The model was applied to real operational data collected over a representative period, to predict the ACS performance and assess its exergy efficiency. For the analysis, input datasets were obtained from the SCADA system, covering hourly measurements over the month of August 2024. These datasets included three groups of parameters that characterise the quality and quantity of the IP steam driving the ACS: pressure, temperature and mass flow rate. The collected input data were used as inputs for the ANN absorption unit, to predict the corresponding cooling capacity and to conduct the exergy analysis. The detailed input datasets are presented in Fig. 5.

From Fig. 5 (a), it is evident that the pressure dynamics of the IP steam driving the ACS fluctuate within the range of 0.83 MPa to 0.87 MPa, with a mean value of 0.85 MPa. The temperature of the IP steam, shown in Fig. 5 (b), varied between 430 K and 490 K, with an average of 469 K. Additionally, the IP steam mass flow rate, depicted in Fig. 5 (c), ranged from 0.04 kg/s to 0.09 kg/s, with a mean value of 0.06 kg/s. The thermal performance results predicted by the machine learning algorithm for the ACS are presented in Fig. 6.

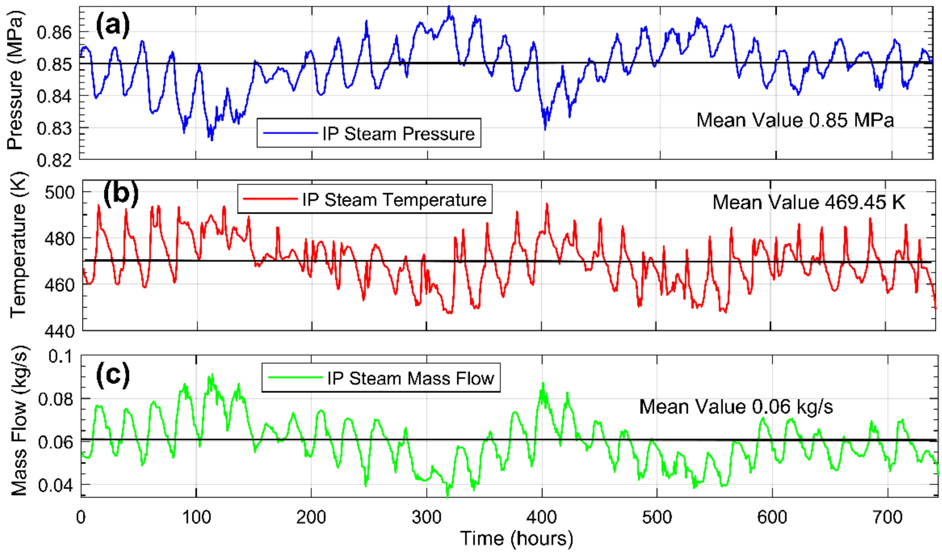

Figure 5: Input data sets for driving the ACS: (a) pressure of the IP steam, (b) temperature of the IP steam, and (c) mass flow rate of the IP steam

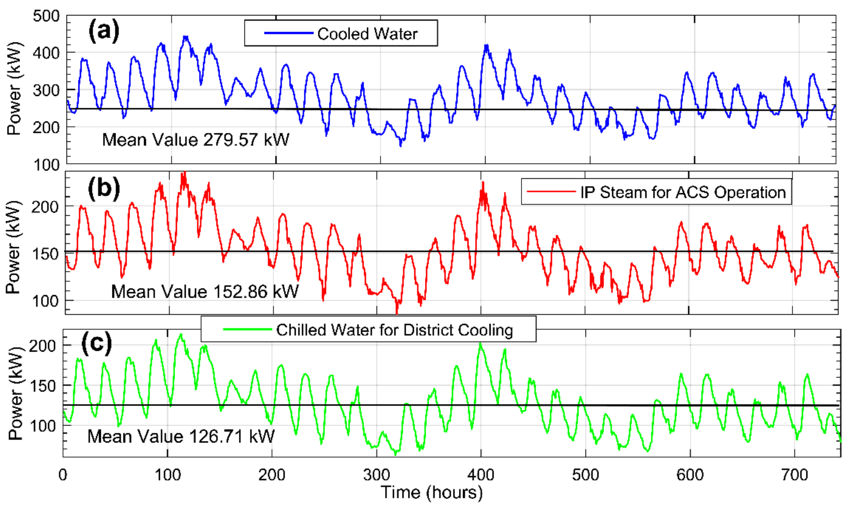

Figure 6: Thermal balance results of the machine learning model for the ACS: (a) cooling power of the chilled water, (b) thermal power of the IP steam for ACS operation, and (c) thermal power of the chilled water

From Fig. 6 (a), it is evident that the thermal power of the cooled water fluctuates within the range of 160 kW to 450 kW, with an average value of 279.57 kW. This thermal energy is utilised for heating demineralised water, which is, subsequently, used as process water in thermal power plant operations. Fig. 6 (b) illustrates the thermal power of the IP steam supplied to the ACS, which varied between 90 kW and 250 kW, with an average of 152.86 kW. Fig. 6 (c) presents the thermal power of the chilled water produced for district cooling, showing values ranging from 68 kW to 207 kW, with a mean of 126.71 kW. Additionally, the machine learning algorithm estimated the thermodynamic exergy values of the ACS, as illustrated in Fig. 7.

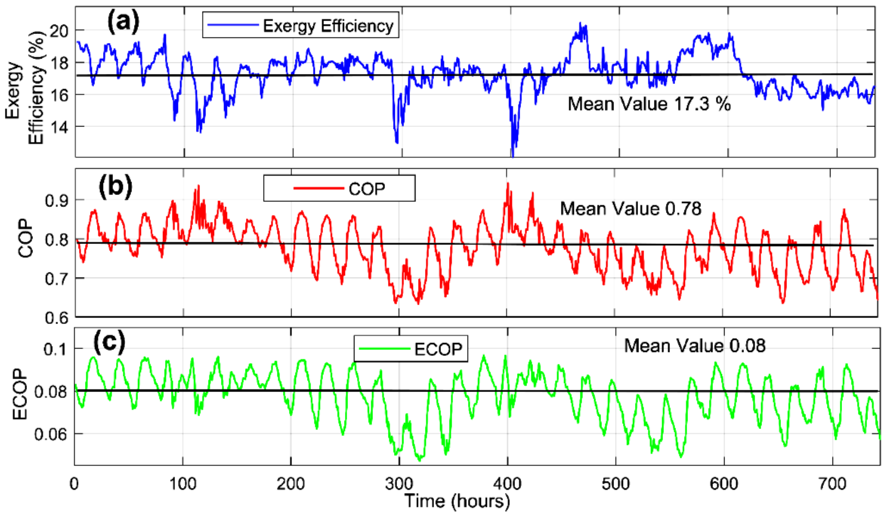

Figure 7: Results of the machine learning algorithm for the ACS: (a) Exergy efficiency; (b) Coefficient of performance (COP); and (c) The exergetic coefficient of performance (ECOP)

Fig. 7 (a) presents the results of the machine learning algorithm for the ACS exergy efficiency. During the analysis period, the exergy efficiency fluctuated between 12% and 20%, with an average value of 17.3%. Fig. 7 (b) shows the COP of the ACS, which varied from 0.65 to 0.9, with a mean value of 0.78 over the analysis period. The machine learning algorithm also calculated the exergetic ECOP, as illustrated in Fig. 7 (c). The ECOP fluctuated within the range of 0.04 to 0.09, with an average value of 0.08 during the analysis period.

4 Conclusions

This article presented a thermal analysis of an ACS using a machine learning approach. A machine-learning model was developed based on real process data collected from an operational ACS. The model's accuracy and reliability were verified through a thorough validation procedure. The results of the machine learning algorithm showed that, during the analysed period, the ACS generated an average of 126.71 kW of cooling for district cooling and 279.57 kW of thermal energy for heating demineralised water. On average, the ACS consumed 0.06 kg/s of intermediate-pressure (IP) steam for its operation. Furthermore, the ACS operated with an average exergy efficiency of 17.3%, an average COP of 0.78, and an average ECOP of 0.08. The average exergy efficiency of the ACS could be improved further by utilising lower-quality operation steam, or even hot water as the driving source, thus enhancing overall system sustainability and performance.

References

[1] Hassan M., El-Sharkawy I. I., Harby K., Study of an innovative combined absorption-adsorption cooling system employing the same evaporator and condenser, *Case Studies in Thermal Engineering*, Vol. 42, p 102690, 2023.

[2] Supervisory Control and Data Acquisition (*SCADA*), URL: http://www.energetika-lj.si.

[3] Park S., Choi H. W., Lee J, W., Cho H. U., Lee N. S., Tae Kang Y. T., Performance analysis of ionic liquids for simultaneous cooling and heating absorption system, *Energy*, Vol. 271, p 127005, 2023.

[4] Strušnik D., Avsec J., Exergoeconomic machine-learning method of integrating a thermochemical Cu–Cl cycle in a multigeneration combined cycle gas turbine for hydrogen production, *International Journal of Hydrogen Energy*, Vol. 47, No. 39, pp 17121-17149, 2022.

[5] Broad air conditioner, Broad two-stage steam chiller BS50., URL; http://en.broad.com/Products-7.aspx

[6] Li G., Zhao S., Wu J., Li C., Liu Y., DV-Hop Localization Algorithm Based on Minimum Mean Square Error in Internet of Things, *Procedia Computer Science*, Vol. 147, pp 458–462, 2019.

[7] Yang L., Entchev E., Performance prediction of a hybrid microgeneration system using Adaptive Neuro-Fuzzy Inference System (ANFIS) technique, *Applied Energy*, Vol. 134, pp 197-203, 2014.

[8] Zueco J., López-Asensio D., Fernández F. J., López-González L. M., Exergy analysis of a steam-turbine power plant using thermocombustion, *Applied Thermal Engineering*, Vol. 180, p 115812, 2020.

[9] Tahaineh H., Frihat M. H., Al-Rashdan M., Al-Tahaineh A., Exergy Analysis of a Single-Effect Water-Lithium Bromide Absorption Chiller Powered by Waste Energy Source for Different Cooling Capacities, *Energy and Power*, Vol. 30, No. 6, pp 106-118, 2020.

[10] Bhurat S. S., Pasupuleti S. R., Kunwer R., Gugulothu S. K., Joshi A., Technical challenges and opportunities for milk chilling unit based on vapor absorption refrigeration systems, *Materials Today: Proceedings*, Vo. 69, No. pp 482-487, 2022.

[11] Chao Fu C., Shen Q., Wu T., Exergo-economic comparisons of solar cooling systems coupled to series/parallel absorption chiller types considering the lowest heat transfer area, *Case Studies in Thermal Engineering*, Vo. 39, p, 102456, 2022.

Nomenclature

Abbreviations

(Symbols)	(Symbol meaning)
ACS	absorption cooling system
ANN	artificial neural network
AI	artificial intelligence
COP	coefficient of the performance
ECOP	exergetic coefficient of the performance
IP	intermediate pressure
MAPE	mean absolute percentage error
MAE	mean absolute error
MSE	mean square error
R^2	correlation coefficient
RMSE	root mean square error
SCADA	supervisory control and data acquisition

Parameters

(Symbols)	(Symbol meaning)
c_p	specific heat of the chilled water, kJ/(kg K)
e_{chil}	specific exergy of the chilled water needed for district cooling, kJ/kg
e_{cond}	condensate specific exergy, kJ/kg
e_{beh}	specific exergy behind the transformation, kJ/kg
e_{bef}	specific exergy before the transformation, kJ/kg
$e_{chilled}$	useful specific exergy of the chilled water, kJ/kg
$e_{cooling}$	useful specific exergy of the cooled water, kJ/kg
e_{dem}	specific exergy for demineralised water heating, kJ/kg
e_{IP}	specific exergy of the IP steam, kJ/kg
e_{loss}	specific exergy losses, kJ/kg
e_{steam}	specific exergy of the *IP* steam, kJ/kg
e_{usef}	useful specific exergy, kJ/kg
$e_{water\ or\ steam}$	specific exergy of the water or steam, kJ/kg
$h_{steam-in}$	specific enthalpy of the *IP* steam into the *ACS*, kJ/kg
$h_{cond-out}$	specific enthalpy of the condensate from the *ACS*, kJ/kg
$T_{chil-out}$	outlet specific enthalpy of the condensate, kJ/kg
$h_{water\ or\ steam}$	specific enthalpy of the water or steam, kJ/kg
h_0	specific enthalpy at an ambient state, kJ/kg
$\dot{m}_{chil}$	mass flow of the chilled water, kg/s
$\dot{m}_{dem}$	mass flow of the demineralised water, kg/s
$\dot{m}_{steam}$	*IP* steam mas flow for *ACS* operation, kg/s
P_{el}	electrical power required for the ACS operation, kW
Q_{cold}	useful cold production, kW
Q_{oper}	heat required for the *ACS* operation, kW
$s_{water\ or\ steam}$	specific entropy of the water or steam, kJ/(kgK)
s_0	specific entropy ambient state, kJ/(kgK)
$T_{chil-in}$	inlet temperature of the chilled water, K

$T_{chil-in}$	outlet temperature of the chilled water, K
T_0	ambient temperature, K

Subscripts and Superscripts

(Symbols)	(Symbol meaning)
o_j	output value
p	pattern
t_j	target value
η_{ex}	exergy efficiency

Povzetek v slovenskem jeziku

Eksergijska analiza absorpcijskega hladilnega sistema z umetno inteligenco. V tem prispevku je predstavljena eksergijska analiza absorpcijskega hladilnega sistema, ki temelji na umetni inteligenci in deluje na principu hladilnega cikla litijev bromid–voda. Za absorpcijski hladilni sistem je značilno, da za svoje delovanje izkorišča srednjetlačno odjemno paro iz parne turbine. Eksergijska analiza umetne inteligence temelji na modelu strojnega učenja, ki napoveduje in optimizira delovanje absorpcijskega hladilnega sistema. Algoritem strojnega učenja je validiran z uporabo realnih procesnih podatkov. Rezultati kažejo, da absorpcijski hladilni sistem generira 126,71 kW hladu za daljinsko hlajenje in 279,57 kW toplote, ki se porabi za ogrevanje demineralizirane vode. V analiziranem obdobju je absorpcijski hladilni sistem v povprečju porabil 152,86 kW srednjetlačne pare in deloval s povprečnim eksergijskim izkoristkom 17,3 %. Študija nakazuje, da bi lahko eksergijski izkoristek hladilnega sistema izboljšali z uporabo manj kakovostne pogonske pare ali celo z uporabo vroče vode.